Journal of ELECTRONIC MATERIALS, Vol. 37, No. 5, 2008
DOI: 10.1007/s11664-008-0385-8

Optical Hall Effect in Hexagonal InN

T. HOFMANN,[1,4] V. DARAKCHIEVA,[2] B. MONEMAR,[2] H. LU,[3] W.J. SCHAFF,[3] and M. SCHUBERT[1]

1.—Department of Electrical Engineering and Nebraska Center for Materials and Nanoscience, University of Nebraska-Lincoln, Nebraska, USA. 2.—Department of Physics, Chemistry and Biology, Linköping University, Linkoping, Sweden. 3.—Department of Electrical and Computer Engineering, Cornell University, Ithaca, USA. 4.—e-mail: thofmann@engr.unl.edu

Measurements of the optical Hall effect in naturally doped high-quality wurtzite-structure InN thin films by generalized ellipsometry reveal that both the surface and the interior (bulk) free electron densities decrease with power-law dependencies on the film thickness. We discover a significant deviation between the bulk electron and dislocation densities. This difference is attributed here to the existence of surface defects with activation mechanism different from bulk dislocations and identifies the possible origin of the so far persistent natural *n*-type conductivity in InN. We further quantify the anisotropy of the Γ-point effective mass.

Key words: InN, electronic properties, electron effective mass, infrared and THz magneto-optic ellipsometry

INTRODUCTION

While common agreement on the band-gap properties of InN has been achieved, the doping and transport mechanisms in InN are still highly unclear.[1–3] InN grown by molecular-beam epitaxy or metalorganic vapor phase deposition techniques is intrinsically *n*-conductive and the lowest intrinsic electron density reported so far was achieved using molecular-beam epitaxy (MBE) with approximately 10^{17} cm^{-3}.[4] In addition to the intrinsic *n*-type conductivity an electron accumulation layer is formed on InN thin-film surfaces.[4–6]

It is well known that continued InN growth decreases both the thin-film conductivity as well as the thin-film dislocation density.[1–3,7] Furthermore, it was shown that conductivity and dislocation densities correlate with similar power-law dependencies on the film thickness.[4,8] The density of threading dislocations scales with a power-law dependence on the InN film thickness in the range $300\,nm \lesssim d_{InN} \lesssim 1400\,nm$.[4] The bulk free electrons may originate from positively charged point defects and threading dislocations.[4,9]

(Received August 1, 2007; accepted January 7, 2008; published online February 2, 2008)

So far, a quantitative assessment of the surface charge accumulation and their origin as a function of thickness and bulk electron density has not been reported. The surface charge accumulation layer presents an immanent complication in the contact-based electrical investigation of free charge carrier properties in InN. The physical origin of the surface charge accumulation and the persistent bulk *n*-type conductivity are still under strong debate. The unknown surface charge accumulation and electric contact potential properties constrain experimental access to the intrinsic electron and hole properties by electrical charge transport measurements.[4,8,10–12]

Here, we report on a new, alternative optical approach to investigate the free charge carrier properties in InN. The precise measurement of the optical Hall effect using magneto-optical generalized ellipsometry (MOGE) at infrared and THz wavelengths allows the determination of the carrier type, density, mobility, and effective mass, and their internal distribution within individual layers and interfaces of semiconductor heterostructures is determined independently by comparison of experimental with best-match model calculations.[13–16] The principle of an optical Hall-effect measurement is shown in Fig. 1. The term optical Hall-effect

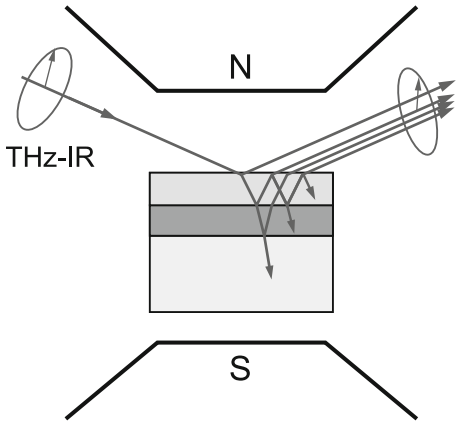

Fig. 1. The principle of an optical Hall-effect measurement. Magneto-optical generalized ellipsometry (MOGE) at infrared and THz wavelengths is used for precise measurement of the optical Hall effect in layered semiconductor heterostructures. The experimental MOGE setup and data analysis are detailed in Ref. 13.

refers to the interaction between long-wavelength electromagnetic radiation and bound and unbound electrical charge carriers subjected to an external magnetic field that causes optical birefringence. The optical birefringence can be precisely determined using MOGE, which measures the polarization response of layered samples within the Mueller matrix descriptor system. This new method is ideally suited for unambiguous separation of the bulk and surface free charge carrier properties in InN thin films. In contrast to electrical capacitance, current, and Hall-effect measurements the IR-MOGE experiment does not require contacts and determines free charge carrier properties in semiconductor layer structures.

EXPERIMENT

A set of naturally n-type InN samples of different thickness ranging from 500 nm to 1600 nm was investigated. The InN epilayers were grown by molecular-beam epitaxy on c-plane sapphire. The high-quality structural properties and low conductivity are achieved by AlN and GaN nucleation layer sequences.[17] Standard X-ray analysis and electrical Hall-effect measurements were employed for structural and electrical characterization.[17] Field-free (standard) IR ellipsometry (IRSE) Ψ- and Δ-spectra of all samples were collected at $\phi = 70^\circ$ angle of incidence. IR-MOGE experiments were carried out at $\phi = 45^\circ$ with samples exposed to fields $\mu_0 H$ = +4.5 T and $\mu_0 H$ = −4.5 T. For further, in-depth description of the MOGE setup and the employed data analysis scheme the interested reader is referred to Ref. 13. All spectra were measured at room temperature. We combined all data within a stratified layer model data analysis. The parameters of the model dielectric functions and layer thickness were varied until the measured and calculated IRSE and MOGE data were simultaneously matched.[18] Anisotropic parametric dielectric functions with Lorentzian line shapes account for the transverse (TO) and longitudinal optic (LO) phonon and high-frequency dielectric polarizability contributions of sapphire (substrate), GaN, AlN (nucleation layers), and InN.[16,19] The free electron magneto-optic birefringence in the InN thin films, detected by the MOGE technique in terms of the anisotropic Mueller matrix element spectra M_{23} and M_{32}, was rendered by the Drude free electron model calculated independently for each differently conducting sheet parallel to the surface of the InN layer. The Drude model provides access to the unscreened plasma frequency $(\omega_p^{*2})_j = Ne^2/(\varepsilon_0 m_j^*)$, the cyclotron frequency $\omega_{c,j} = q\mu_0 H/(m_j^*)$, and the plasmon damping parameter $\gamma_{p,j} = q/(\mu_j m_j^*)$ for polarization j = "$\parallel$", "$\perp$" to the InN c-axis,[13,20] which easily converts into the electron density N, effective mass m_j^*, and the mobility μ_j parameters (ε_0 and μ_0 are the vacuum permittivity and permeability, respectively; $q = -|e|$ is the elementary charge).

RESULTS AND DISCUSSION

Figure 2 shows all relevant experimental and best-model calculated IRSE spectra in the spectral range from 375 cm^{-1} to 1200 cm^{-1}. The spectra are dominated by sapphire phonon and interface polariton resonances,[21] and by the coupled longitudinal phonon-plasmon resonance caused by the bulk InN electron plasma and LO phonon excitation (cf. Fig. 1 in Ref. 22). The bulk electron density in the InN films increases from top $(1.91 \pm 0.12 \times 10^{17}\,cm^{-3})$ to bottom $(8.55 \pm 0.03 \times 10^{18}\,cm^{-3})$ in Fig. 2. The errors of the best-model electron density parameters correspond to a 90% confidence interval of the fit procedure. Subtle resonances identify the InN $E_1(478\,cm^{-1})$ and $A_1(443\,cm^{-1})$ TO phonon modes. Figure 3 presents MOGE spectra in the range from 200 cm^{-1} to 650 cm^{-1}. The data are differences between the Mueller matrix spectra measured at $\mu_0 H$ = +4.5 T and those measured at $\mu_0 H$ = −4.5 T. The magneto-optic polarization coupling is strongest at $\omega \sim 450\,cm^{-1}$, which is the spectral location of the interface modes caused by the InN thin film/buffer interface, and which depend nonlinearly on the thickness and bulk electron concentration.[21] The magnitude of the MOGE spectra, as expected, reduce with decreasing bulk carrier concentration.

In a previous publication we discussed the results for the InN phonon and plasmon mode frequencies and damping parameters from the field-free measurements.[19] In this report we use MOGE measurements for precise differentiation between the two different free electron density contributions within the InN samples. Furthermore, the electron effective mass parameter, including its anisotropy, can be quantified. We find, that the InN thin film is composed of a very thin surface layer with a

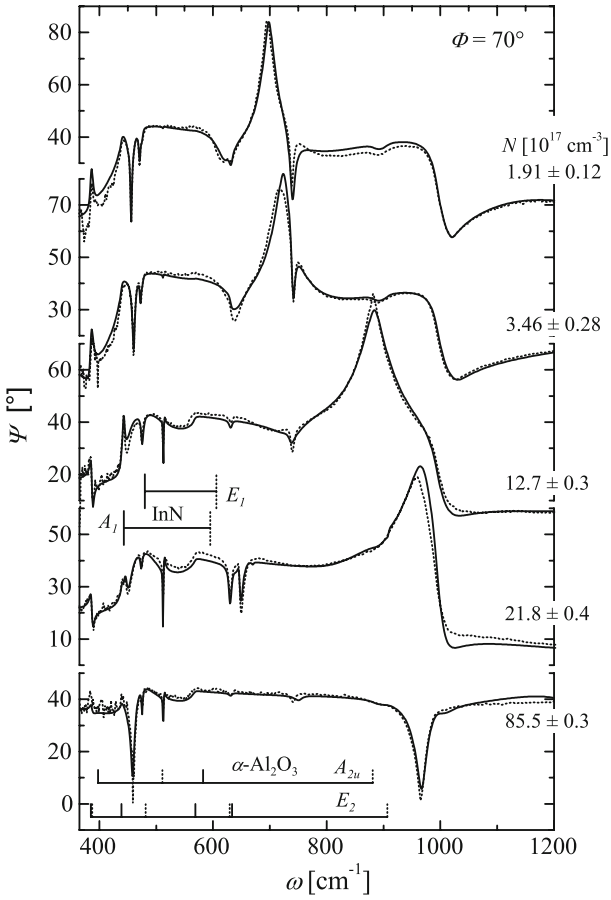

Fig. 2. Field-free ($\mu_0 H = 0$) experimental (dotted) and best-model calculated (solid lines) IRSE Ψ spectra from InN thin films deposited on *c*-plane sapphire with varying thickness and free electron density.

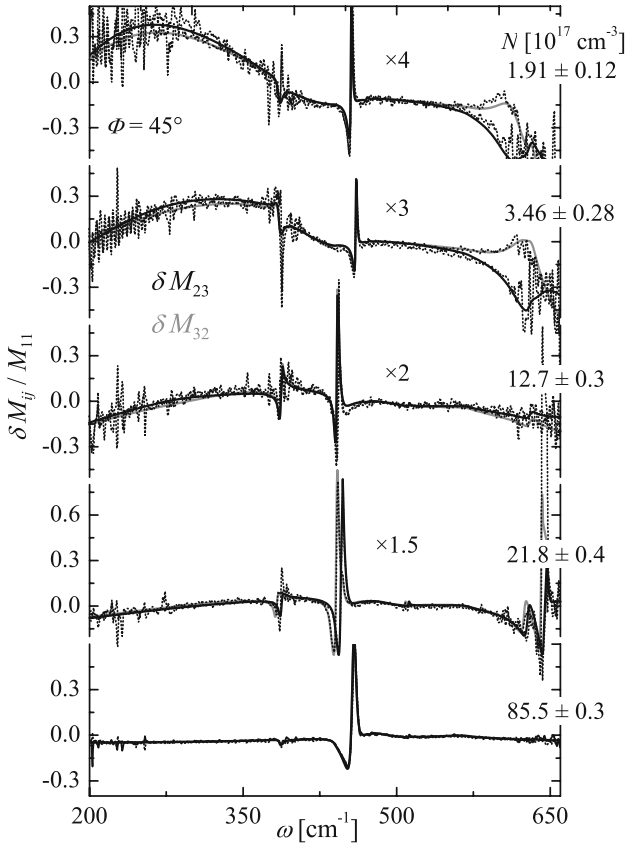

Fig. 3. Experimental (dotted lines) and best-model (solid lines) MOGE difference spectra δM_{23} and δM_{32} taken between M_{23}, M_{32} obtained at $\mu_0 H = -4.5$ T and M_{23} and M_{32} at $\mu_0 H = +4.5$ T, respectively.

thickness of 3 nm to 5 nm and bulk (the remaining part of the InN thin film). Phonon and high-frequency contributions are identical in both InN sheets, except for the free electron density.

Figure 4 depicts the parallel and perpendicular electron effective mass parameters as a function of the InN bulk electron density. We have included previous experimental data obtained from infrared studies and electrical Hall-effect analysis for comparison. A significant anisotropy for $N < 10^{19}$ cm^{-3} can be observed from our MOGE data (○ and • in Fig. 4). We find that the out-of-plane mass $m_\perp^*$ is larger then the in-plane mass $m_\parallel^*$. Kane's two-band kp model, upon comparison with the effective mass parameters obtained here for both polarizations, predicts for the bottom of the InN conduction band $m_\perp^* = 0.050\, m_0$ and $m_\parallel^* = 0.037\, m_0$. These values are in excellent agreement with very recent *ab initio* band-structure calculations.[23,24] Our observation quantitatively confirms the assumption $m_\perp^* > m_\parallel^*$ concluded qualitatively from anomalous Shubnikov–de Haas oscillations in InN.[25]

The electron densities obtained for bulk and surface charge accumulation layer are shown in Fig. 5

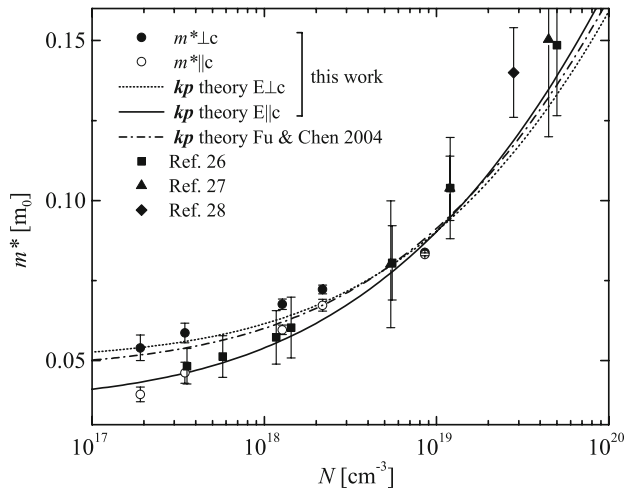

Fig. 4. Effective mass parameters of hexagonal InN for polarization parallel and perpendicular to the *c*-axis obtained from MOGE analysis. Data from previous reports and kp calculations are included for comparison.[26–28]

as a function of the InN film thickness. Both the bulk and the surface charge accumulation densities decrease with increasing thickness in the

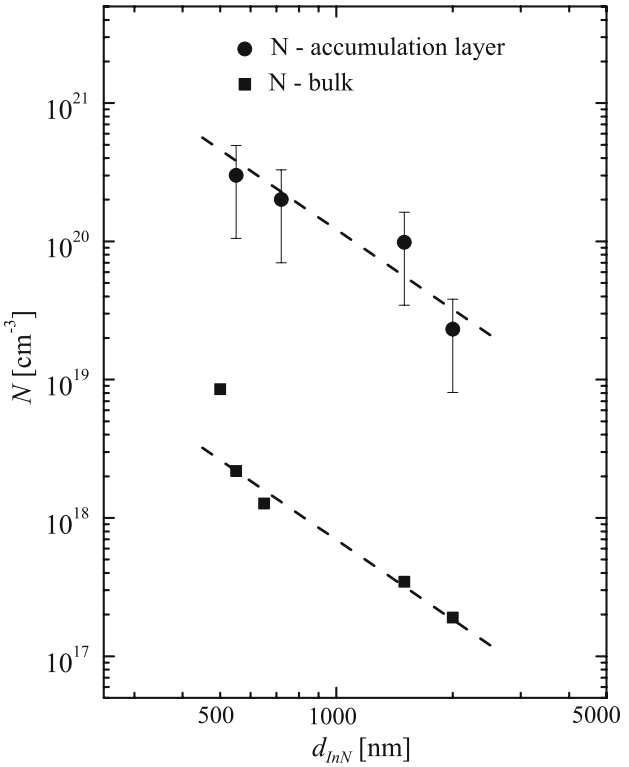

Fig. 5. InN bulk and surface electron accumulation densities as a function of the layer thickness. Both the bulk and the surface electron accumulation density follow the same power law ($N \sim d_{\mathrm{InN}}^{-1.92}$) in the investigated thickness region.

investigated thickness region according to the same power law $N \sim d_{\mathrm{InN}}^{-\alpha}$. We obtain a scaling factor $\alpha = 1.92$. In concordance with recent capacitance–voltage and high-resolution electron-energy-loss spectroscopy investigations we find that the surface electron density is almost two orders of magnitude larger then the bulk density.[6,29,30] While the bulk density dominates current transport for small thicknesses, the surface accumulation dominates conductivity measurement for large thickness, which causes a smaller power law observed by electrical measurements on the thin films, as reported by Arnaudov et al.[12] with $\alpha = 0.7$, or requires exponential modeling over larger thickness ranges.[4,8] According to Cimalla et al.[4] the threading dislocation density in InN follows a different power law: $\sigma_{\mathrm{TD}} \sim d_{\mathrm{InN}}^{-2.7\pm0.3}$ for $300 \lesssim d_{\mathrm{InN}} \lesssim 1400$ nm (cf. Fig. 1 Ref. 4). Assuming a density-independent free electron generation mechanism of the dislocations, the contribution of σ_{TD} to N is proportional to $\mathrm{d}\sigma_{\mathrm{TD}}/\mathrm{d}d_{\mathrm{InN}}$. This suggests a scaling factor for $N \sim d_{\mathrm{InN}}^{-\alpha}$ with $\alpha = -3.7 \pm 0.3$ in this thickness range. It is very obvious from Fig. 5, however, that the bulk density decreases much more slowly with increasing thickness than could be account for by the threading dislocations. Thus we conclude that an additional thickness-dependent donor mechanism must exist in naturally n-type InN. This mechanism contributes to both the bulk and surface electron accumulation density inversely proportionally to the square of the thickness. Our observation corroborates earlier findings of two different kinds of donors when implant-damaged and annealed material was studied.[31]

The bulk electron mobility decreases linearly in double-log scale with increasing density from 1600 cm^2/(V s) to 800 cm^2/(V s), concordant with dominant ionized-impurity or donor-site scattering mechanisms. We also observe that $\mu_{\parallel} > \mu_{\perp}$, which we account for by additional scattering across grain boundaries.

It is currently assumed that the electron accumulation layer originates from the low conduction-band minimum of InN at the Γ-point, which permits efficient ionization of donor-type surface states inside the conduction band.[32,33] These states emit their electrons into the conduction band and acquire positive charges, which are then compensated by an accumulation of electrons close to the surface. This view is in agreement with our result here if the origin of the surface states are taken into consideration.

The scenario favored here includes the ionized surface states as the restoring force, and point-defect-generated surface states. The ionization efficiency of a near-surface point defect is larger by two orders of magnitude than within the bulk. Further surface charge may originate from internal wurtzite-structure spontaneous and near-surface piezoelectric polarization fields, which requires further investigation.

CONCLUSION

We used magneto-optic generalized ellipsometry in the infrared–THz spectral domain for the measurement of the optical Hall effect in wurtzite-structure InN thin-film samples. We separated bulk and surface electron accumulation properties by noncontact optical means. A common power-law density dependency on the InN film thickness was found. A strong difference between the scaling factors of the true bulk electron density and previously counted dislocation densities proves the existence of an additional doping mechanism. Point defects, previously thought to be thickness independent, are most likely the origin of this behavior. As a consequence it might be easier to neutralize surface donors in InN when the background electron density is also low. This finding could be tested by introducing electrons by damage such as ion bombarding and subsequent annealing processes. The InN Γ-point effective mass is found to be highly anisotropic: $m_{\perp}^{*} = 0.050 \pm 0.03\, m_0$ and $m_{\parallel}^{*} = 0.037 \pm 0.03\, m_0$ for the polarizations perpendicular and parallel to the c-axis, respectively.

ACKNOWLEDGEMENTS

M.S. acknowledges startup funds from the College of Engineering at University of Nebraska–Lincoln, support from the J.A. Woollam Foundation,

and the National Science Foundation in MRSEC QSPIN. T.H. and M.S. also thank Craig M. Herzinger with J.A. Woollam Co., Inc. for many fruitful discussions.

REFERENCES

1. H. Lu, W.J. Schaff, J. Hwang, H. Wu, W. Yeo, A. Pharkya, and L.F. Eastman, *Appl. Phys. Lett.* 77, 2548 (2000).
2. C.H. Swartz, R.P. Tomkins, T.H. Myers, H. Lu, and W.J. Schaff, *Phys. Stat. Sol. (c)* 2, 2250 (2005).
3. C.S. Gallinat, G. Koblmüller, J.S. Brown, S. Bernardis, J.S. Speck, G.D. Chern, E.D. Readinger, H. Shen, and M. Wraback, *Appl. Phys. Lett.* 89, 032109 (2006).
4. V. Cimalla, V. Lebedev, F.M. Morales, R. Goldhahn, and O. Ambacher, *Appl. Phys. Lett.* 89, 172109 (2006).
5. D.C. Look, H. Lu, W.J. Schaff, J. Jasinski, and Z. Liliental-Weber, *Appl. Phys. Lett*. 80, 258 (2002). ISSN 00036951.
6. I. Mahboob, T.D. Veal, C.F. McConville, H. Lu, and W.J. Schaff, *Phys. Rev. Lett.* 92, 036804 (2004).
7. F. Chen, A.N. Cartwright, H. Lu, and W.J. Schaff, *J. Cryst. Growth* 269, 10 (2004).
8. V. Lebedev, V. Cimalla, T. Baumann, O. Ambacher, F. Morales, J. Lozano, and D. Gonzalez, *J. Appl. Phys.* 100, 94903 (2006).
9. L.F.J. Piper, T.D. Veal, C.F. McConville, H. Lu, and W.J. Schaff, *Appl. Phys. Lett.* 88, 252109 (2006).
10. H. Lu, W. Schaff, L. Eastman, and C. Stutz, *Appl. Phys. Lett.* 82, 1736 (2003).
11. C. Swartz, R. Tompkins, N. Giles, T. Myers, H. Lu, W. Schaff, and L. Eastman, *J. Cryst. Growth* 269, 29 (2004).
12. B. Arnaudov, T. Paskova, S. Evtimova, B. Monemar, H. Lu, and W.J. Schaff, *Phys. Stat. Sol. (a)* 203, 1681 (2006).
13. T. Hofmann, U. Schade, W. Eberhardt, C. Herzinger, P. Esquinazi, and M. Schubert, *Rev. Sci. Inst.* 77, 63902 (2006).
14. T. Hofmann, M. Schubert, C.M. Herzinger, and I. Pietzonka, *Appl. Phys. Lett.* 82, 3463 (2003).
15. M. Schubert, *Infrared Ellipsometry on Semiconductor Layer Structures: Phonons, Plasmons and Polaritons, vol. 209 of Springer Tracts in Modern Physics* (Berlin: Springer, 2004).
16. M. Schubert, T. Hofmann, and C.M. Herzinger, *J. Opt. Soc. Am. A* 20, 347 (2003).
17. H. Lu, W.J. Schaff, J. Hwang, H. Wu, G. Koley, and L.F. Eastman, *Appl. Phys. Lett.* 79, 1489 (2001).
18. G.E. Jellison, *Thin Solid Films* 313–314, 33 (1998).
19. V. Darakchieva, P.P. Paskov, E. Valcheva, T. Paskova, B. Monemar, M. Schubert, H. Lu, and W.J. Schaff, *Appl. Phys. Lett.* 84, 3636 (2004).
20. C. Pidgeon, *Handbook on Semiconductors*, ed. M. Balkanski (North-Holland, Amsterdam, 1980).
21. M. Schubert, T. Hofmann, and J. Šik, *Phys. Rev. B* 71, 35324 (2005).
22. A. Kasic, M. Schubert, S. Einfeldt, D. Hommel, and T.E. Tiwald, *Phys. Rev. B* 62, 7365 (2000).
23. P. Carrier and S.-H. Wei, *J. Appl. Phys.* 97, 33707 (2005).
24. P. Rinke, M. Scheffler, A. Qteish, M. Winkelnkemper, D. Bimberg, and J. Neugebauer, *Appl. Phys. Lett.* 89, 161919 (2006).
25. T. Inushima, M. Higashiwaki, T. Matsui, T. Takenobu, and M. Motokawa, *Phys. Rev. B* 72, 85210 (2005).
26. S. Fu and Y. Chen, *Appl. Phys. Lett.* 85, 1523 (2004).
27. J. Wu, W. Walukiewicz, K.M. Yu, J.W. Ager, E.E. Haller, H. Lu, W.J. Schaff, Y. Saito, and Y. Nanishi, *Appl. Phys. Lett.* 80, 3967 (2002).
28. A. Kasic, M. Schubert, Y. Saito, Y. Nanishi, and G. Wagner, *Phys. Rev. B* 65, 115206 (2002).
29. H. Lu, W.J. Schaff, L.F. Eastman, J. Wu, W. Walukiewicz, V. Cimalla, and O. Ambacher, *Appl. Phys. Lett.* 83, 1136 (2003).
30. L. Piper, T. Veal, I. Mahboob, C. McConville, H. Lu, and W. Schaff, *Phys. Rev. B* 70, 115333 (2004).
31. R. Jones, H. van Genuchten, S. Li, L. Hsu, K. Yu, W. Walukiewicz, J.W. Ager, E. Haller, H. Lu, W. Schaff et al., *Mat. Res. Soc. Symp. Proc.* 892, 105 (2006), ISSN 1 55899 846 2.
32. I. Mahboob, T.D. Veal, L.F.J. Piper, C.F. McConville, H. Lu, W.J. Schaff, J. Furthmüller, and F. Bechstedt, *Phys. Rev. B* 69, 201307 (2004).
33. S.X. Li, K.M. Yu, J. Wu, R.E. Jones, W. Walukiewicz, J.W. Ager III, W. Shan, E.E. Haller, and H. Lu et al., *Phys. Rev. B* 71, 161201 (2005).